# *Supporting Information for*:

## Isolation and characterization of a new polyoxometalate ligand, $H_3SbW_{14}O_{50}^{10-}$, and its interactions with *f*-elements.

Ian Colliard[a,b]* and Gauthier J.-P. Deblonde[a,c]*

[a] *Physical and Life Sciences Directorate, Glenn T. Seaborg Institute, Lawrence Livermore National Laboratory, Livermore, California 94550, USA*

[b] *Material Sciences Division, Lawrence Livermore National Laboratory, Livermore, California 94550, USA*

[c] *Nuclear and Chemical Sciences Division, Lawrence Livermore National Laboratory, Livermore, California 94550, USA*

## Experimental Section

*Precaution: all isotopes for curium are highly radioactive and toxic! Extreme caution and appropriate procedures should be taken. All experiments involving radionuclides were conducted at Lawrence Livermore National Laboratory, in facilities designed for the safe handling of long-lived and short-lived radioactive materials and associated waste.*

**Materials:** Curium samples (97% $^{248}Cm$ + 3% $^{246}Cm$ + 0.01% $^{247}Cm$) were prepared from a primary source purchased from Oak Ridge National Laboratory (USA), and $^{243}Am$(III) chloride purchased from Eckert & Ziegler (USA). $Sb_2O_3$ (>99.99%), and $NaCH_3COO$ (≥99.9%), cesium chloride (>99.99%), $Na_2WO_4{\cdot}2H_2O$ (≥99%), phosphoric acid, and lanthanide trichloride salts (europium and neodymium) (>99.9%) were purchased from chemical providers (VWR and Millipore Sigma) and used as received. All solutions were prepared using deionized water purified by reverse osmosis cartridge system (≥ 18.2 MΩ.cm). All experiments were performed in a temperature-controlled room (22°C).

**Synthesis of $SbW_9$ and $SbW_{14}$ POMs.**

**$SbW_9$:** This precursor was synthesized using the protocol previously reported by Bösing et al.[1] Briefly, this POM was prepared by dissolving $Na_2WO_4$ $2H_2O$ (40 g, 121 mmol) in boiling water (80 mL) and drop wise addition of $Sb_2O_3$ (1.96 g,6.72 mmol) dissolved in concentrated HCI (10 mL). The mixture was refluxed for 1 h and allowed to cool slowly. The volume of the solution was halved, at which point 10 g of NaCl is added, $NaSbW_9$ and $Na_9SbW_9O_{33}nH_2O$ precipitated out. The solids were collected and washed. (1, 2). Selected Raman peaks ($cm^{-1}$); 958, 940, 874, 239, 219, 107, and 89. Selected IR peaks ($cm^{-1}$); 743, 695, 660, 623, 520, and 440.

**$SbW_{14}$:** was prepared by dissolving 30 mg of $SbW_9$ in 5 mL of acetate buffer (0.1 M at pH = 5.5). An additional 5 mL of 6 M CsCl is added the solution. The solution, with a total volume of 10 mL, is left uncapped. After 24hrs crystals of $SbW_{14}$ appeared, after which they were harvested and characterized. Selected Raman peaks ($cm^{-1}$); 958, 940, 904, 225, 179, 151, and 109. Selected IR peaks ($cm^{-1}$); 724, 694, 651, and 444.

**Raman Microscopy.** Raman spectra were collected using a Senterra II confocal Raman microscope (Bruker), equipped with high resolution gratings (1,200 lines/mm) and a 532 nm laser source (operated at 15 mW), and a TE-cooled CCD detector. Reported spectra are the average of at least 2-5 different spots per sample, each spot analysis consisting of 16 scans. The integration time was set to 400 ms per scan. No damage to the sample was observed due to the laser irradiation.

**FTIR.** Infrared spectra were collected using a Cary 630 FTIR instrument (Agilent Technologies) equipped with an attenuated total reflectance (diamond ATR) cell.

**UV-visible spectrophotometry ($Nd^{3+}$ and $Am^{3+}$).** Absorbance spectra of the Am(III) and Nd(III) samples were measured using a high-performance Cary 6000i UV-vis-NIR spectrophotometer (Agilent Technologies). Samples were contained in quartz cuvettes with a 10 mm path length. Spectra were blank corrected by measuring the absorbance of the corresponding buffer prior to the samples.

**Fluorescence spectroscopy ($Eu^{3+}$ and $Cm^{3+}$)**. Steady-state fluorescence spectra and fluorescence lifetimes were measured with a FLS1000 spectrometer (Edinburgh Instruments) equipped with a double monochromator on the excitation arm and emission arm. A 450 W Xenon lamp was used as light source for the steady-state measurements and a 60 W microsecond flashlamp was used for lifetime measurements (MCS mode). Each lifetime decay curve contains 2,000 data points, with the maximum count per channel set to at least 1,000. The timespan of the acquisition was set so that the signal was measured until its return to background level. Lifetimes were calculated based on the dataset fit using the Fluoracle computer program (Edinburgh Instruments). Fluorescence data for liquid samples were measured in sealed quartz cuvettes, and the emission was collected at 90° relative to the excitation.

**Dynamic light scattering (DLS).** DLS measurements were performed using Zetasizer Nano ZS instrument (Malvern Instruments) in backscatter detection mode. Samples were prepared in the same buffer used for fluorescence and UV-vis experiments (acetate 0.1 M at pH = 5.5). At least 10 acquisitions were performed for each DLS curve. The hydrodynamic diameters reported in this study were calculated based on the volume distribution using the Zetasizer Explorer software (Malvern).

**Crystallographic studies.** The structure of $SbW_{14}$ was collected at LLNL's radiochemistry laboratories using a Rigaku Synergy Custom single crystal diffractometer, equipped with a kappa goniometer and using Mo Kα radiation (λ = 0.71073 Å) with a FWHM of ~200 μm at the sample from a MicroMax-007 HF microfocus rotating anode source. Images were recorded on a Dectris Pilatus 3R (300K – CdTe) detector and processed using CrysAlis$^{Pro}$. After integration both analytical absorption and empirical absorption (spherical harmonic, image scaling, detector scaling) corrections were applied.[3] All structures were solved by Intrinsic Phasing method from SHELXT program[4], developed by successive difference Fourier syntheses, and refined by full-matrix least square on all $F^2$ data using SHELX[5] via OLEX2 interface.[6]

Crystallographic information for the six reported structures can be obtained free of charge from the Cambridge Crystallographic Data Center (https://www.ccdc.cam.ac.uk/) upon referencing CCDC numbers in the crystallographic tables below.

**Notes on crystal structures, refinement, modeling of disorder, and solvent void space**

Some crystals exhibit solvent accessible void-space, where a solvent mask was applied to calculate the electron density and this the number of disordered water molecules that could not be

individually refined. In each case, the electron count was in good agreement with the solvent accessible void volume, assuming 30 - 40 $Å^3$ per water molecule (7-9). As such the electron count was used to describe the solvent mask. Any residual q-peaks are from after the application of the solvent mask. Based on the solvent mask result, 3 hydrate water molecules were masked for a total of 6 waters.

**Common cif alerts and responses thereof**

- **PLAT971/2/3_ALERT_2_A Check Calcd Resid. Dens. X Ang from X**
  Response: High residual Q-peaks of 0.1*Z/$Å^3$ at 0.6 – 1.2 Å away from the heavy atoms (10). While most structures are within this range, we nevertheless processed the data through several different absorption correction methods before ultimately using spherical or multi-scan methods. (10)
- **PLAT910_ALERT_3_B Missing # of FCF Reflection(s) Below Theta(Min).**
  Response: Missing hkl reflection missing due to beam stop mask applied to detector during data collection while at minimal distance allowed by the instrument. As such, a decision was taken to sacrifice a few reflections for higher overall intensity, due to the size and synthesis nature of the crystals.
- **PLAT306_ALERT_2_B Isolated Oxygen Atom (H-atoms Missing ?)**
  Response: solvent water molecules, H-atoms not located.

Table S1. Crystallographic information for $SbW_{14}$

| **Identification code** | **SbW14-Cs** |
|---|---|
| **Empirical formula** | $H_3Cs_{10}O_{53}SbW_{14}$ |
| **CCDC** | 2326569 |
| **Formula weight** | 4877.76 |
| **Temperature/K** | 298 |
| **Crystal system** | orthorhombic |
| **Space group** | $P2_12_12_1$ |
| **a/Å** | 16.2565(5) |
| **b/Å** | 18.2879(5) |
| **c/Å** | 22.2320(6) |
| **α/°** | 90 |
| **β/°** | 90 |
| **γ/°** | 90 |
| **Volume/Å$^3$** | 6609.5(3) |
| **Z** | 4 |
| **$\rho_{calc}$g/cm$^3$** | 4.898 |
| **μ/mm$^{-1}$** | 30.171 |
| **F(000)** | 8248 |
| **Crystal size/mm$^3$** | 0.05 × 0.01 × 0.01 |
| **Radiation** | MoKα (λ = 0.71073) |
| **2Θ range for data collection/°** | 6.93 to 63.862 |
| **Index ranges** | $-22 \leq h \leq 22$, $-25 \leq k \leq 26$, $-31 \leq l \leq 32$ |
| **Reflections collected** | 108623 |
| **Independent reflections** | 19244 [$R_{int}$ = 0.0874, $R_{sigma}$ = 0.0574] |
| **Data/restraints/parameters** | 19244/0/690 |
| **Goodness-of-fit on F$^2$** | 1.042 |
| **Final R indexes [I>=2σ (I)]** | $R_1$ = 0.0489, $wR_2$ = 0.1286 |
| **Final R indexes [all data]** | $R_1$ = 0.0604, $wR_2$ = 0.1346 |
| **Largest diff. peak/hole / e Å$^{-3}$** | 4.67/-5.28 |
| **Flack parameter** | 0.183(5) |

Table S2. BVS for Sb designation

| Atom1 | Atom2 | Bond Length | BV | BVS |
|---|---|---|---|---|
| **Sb1** | O48 | 2.011 | 0.893162 | 2.648637 |
| | O12 | 2.036 | 0.864629 | |
| | O27 | 2.013 | 0.890845 | |

BVS parameters for Sb: $R_0$ = 1.924 and b = .47 (11)

Table S3. BVS for oxygen designation

| Atom | Atom | Bond Length | BV | BVS | Designation |
|---|---|---|---|---|---|
| **W4** | O1 | 1.828 | 1.28576176 | 1.83 | Oxo |
| **W8** | O1 | 2.147 | 0.54291049 | | |
| **W1** | O10 | 1.95 | 0.92461451 | 1.95 | Oxo |
| **W9** | O10 | 1.913 | 1.02185706 | | |
| **W3** | O11 | 1.74 | 1.63099326 | 1.63 | Oxo |
| **W6** | O12 | 2.339 | 0.32312057 | 1.87 | Oxo |
| **W14** | O12 | 2.259 | 0.40111243 | | |
| **W5** | O12 | 2.247 | 0.41433474 | | |
| **Sb1** | O12 | 2.036 | 0.73285251 | | |
| **W10** | O13 | 1.936 | 0.96027023 | 1.89 | Oxo |
| **W3** | O13 | 1.948 | 0.92962595 | | |
| **W6** | O14 | 1.938 | 0.95509359 | 2.00 | Oxo |
| **W12** | O14 | 1.903 | 1.04985142 | | |
| **W14** | O15 | 1.901 | 1.05554166 | 1.96 | Oxo |
| **W2** | O15 | 1.958 | 0.90483742 | | |
| **W8** | O16 | 1.971 | 0.87359785 | 1.91 | Oxo |
| **W9** | O16 | 1.907 | 1.0385628 | | |
| **W10** | O17 | 1.772 | 1.49586211 | 1.50 | Oxo |
| **W1** | O18 | 1.796 | 1.40191315 | 1.86 | Oxo |
| **W8** | O18 | 2.211 | 0.45667478 | | |
| **W2** | O19 | 1.737 | 1.64427128 | 1.64 | Oxo |
| **W12** | O2 | 1.891 | 1.08445882 | 1.99 | Oxo |
| **W11** | O2 | 1.957 | 0.90728623 | | |
| **W14** | O20 | 1.962 | 0.89510808 | 1.93 | Oxo |
| **W7** | O20 | 1.91 | 1.03017607 | | |
| **W11** | O21 | 1.77 | 1.50396974 | 1.50 | Oxo |
| **W7** | O22 | 1.858 | 1.18562525 | 1.78 | Oxo |
| **W2** | O22 | 2.112 | 0.59677435 | | |
| **W6** | O23 | 1.778 | 1.47180051 | 1.47 | Oxo |
| **W2** | O24 | 1.941 | 0.9473809 | 1.98 | Oxo |
| **W3** | O24 | 1.908 | 1.03575967 | | |
| **W8** | O25 | 1.933 | 0.96808786 | 2.03 | Oxo |
| **W10** | O25 | 1.899 | 1.06126274 | | |
| **W4** | O26 | 2.072 | 0.66490699 | 1.16 | Hydroxo |
| **W3** | O26 | 2.18 | 0.4965853 | | |
| **W1** | O27 | 2.199 | 0.47172865 | 1.94 | Oxo |
| **W12** | O27 | 2.347 | 0.31620917 | | |
| **W7** | O27 | 2.29 | 0.36887505 | | |
| **Sb1** | O27 | 2.013 | 0.77985393 | | |
| **W9** | O28 | 1.684 | 1.89750628 | 1.90 | Oxo |
| **W8** | O29 | 1.76 | 1.54517185 | 1.55 | Oxo |
| **W10** | O3 | 1.73 | 1.67567525 | 1.68 | Oxo |
| **W11** | O30 | 1.863 | 1.16971105 | 1.82 | Oxo |

| | | | | | |
|---|---|---|---|---|---|
| **W13** | O30 | 2.078 | 0.65421167 | | |
| **W13** | O31 | 1.714 | 1.74972645 | 1.75 | Oxo |
| **W1** | O32 | 2.032 | 0.74081822 | 1.89 | Oxo |
| **W12** | O32 | 1.869 | 1.15089574 | | |
| **W6** | O33 | 1.915 | 1.01634841 | 1.91 | Oxo |
| **W14** | O33 | 1.963 | 0.89269213 | | |
| **W4** | O34 | 1.758 | 1.55354675 | 1.55 | Oxo |
| **W14** | O35 | 1.895 | 1.07279809 | 1.90 | Oxo |
| **W5** | O35 | 1.993 | 0.82316831 | | |
| **W8** | O36 | 1.759 | 1.54935364 | 1.55 | Oxo |
| **W13** | O37 | 1.71 | 1.76874503 | 1.77 | Oxo |
| **W4** | O38 | 1.809 | 1.35351201 | 1.90 | Oxo |
| **W2** | O38 | 2.143 | 0.54881164 | | |
| **W6** | O39 | 1.84 | 1.24473035 | 1.86 | Oxo |
| **W5** | O39 | 2.1 | 0.61644647 | | |
| **W9** | O4 | 1.916 | 1.01360523 | 2.04 | Oxo |
| **W11** | O4 | 1.913 | 1.02185706 | | |
| **W2** | O40 | 1.796 | 1.40191315 | 1.40 | Oxo |
| **W6** | O41 | 1.907 | 1.0385628 | 2.08 | Oxo |
| **W11** | O41 | 1.906 | 1.04137353 | | |
| **W9** | O42 | 1.924 | 0.99192467 | 1.81 | Oxo |
| **W13** | O42 | 1.994 | 0.82094653 | | |
| **W14** | O43 | 1.71 | 1.76874503 | 1.77 | Oxo |
| **W7** | O44 | 1.694 | 1.84690915 | 1.85 | Oxo |
| **W12** | O45 | 1.752 | 1.57894477 | 1.58 | Oxo |
| **W5** | O46 | 1.93 | 0.97596913 | 1.93 | Oxo |
| **W13** | O46 | 1.938 | 0.95509359 | | |
| **W3** | O47 | 1.72 | 1.72158132 | 1.72 | Oxo |
| **W9** | O48 | 2.268 | 0.39147335 | 1.89 | Oxo |
| **W11** | O48 | 2.373 | 0.2947518 | | |
| **W13** | O48 | 2.238 | 0.42453673 | | |
| **Sb1** | O48 | 2.011 | 0.78408077 | | |
| **W5** | O49 | 1.742 | 1.62220086 | 1.62 | Oxo |
| **W5** | O5 | 1.74 | 1.63099326 | 1.63 | Oxo |
| **W1** | O50 | 1.763 | 1.53269409 | 1.53 | Oxo |
| **W4** | O6 | 2.1 | 0.61644647 | 1.08 | Hydroxo |
| **W10** | O6 | 2.203 | 0.46665635 | | |
| **W12** | O7 | 1.955 | 0.91220376 | 1.79 | Oxo |
| **W7** | O7 | 1.971 | 0.87359785 | | |
| **W4** | O8 | 2.256 | 0.40437791 | 1.22 | Hydroxo |
| **W10** | O8 | 2.251 | 0.40987957 | | |
| **W3** | O8 | 2.256 | 0.40437791 | | |
| **W1** | O9 | 1.944 | 0.93973049 | 1.79 | Oxo |
| **W7** | O9 | 1.981 | 0.85030331 | | |

BVS parameters for W: $R_0$ = 1.921 and b = .37 (12)

Table S4. Fluorescence lifetime decay fit results for aqueous solutions of $Eu^{3+}$ and $Cm^{3+}$ with $SbW_9$ and $SbW_{14}$. All decay curves were fit with a mono-exponential decay function.

| | | A (parameter) | Lifetime value (ms) | chi2 | Lifetime uncertainty (ms) |
|---|---|---|---|---|---|
| **$Eu^{3+}$** | SbW9 | 1349 | 336 | 1.22 | 0.76 |
| | SbW14 | 173 | 621 | 1.13 | 3.31 |
| **$Cm^{3+}$** | SbW9 | 171 | 132 | 0.83 | 0.74 |
| | SbW14 | 202 | 177 | 0.76 | 0.79 |

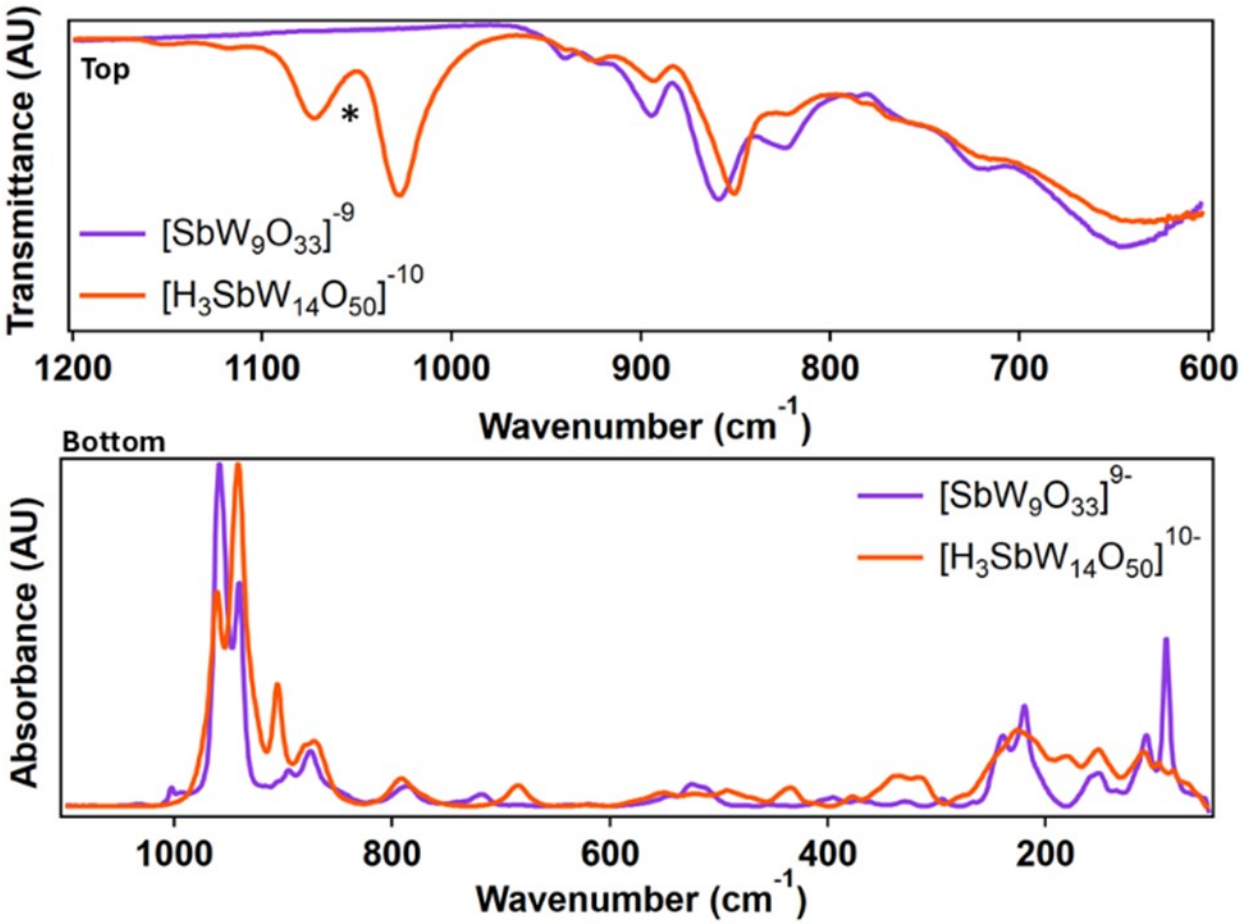


Figure S1. Solid-state vibrational spectroscopies on $SbW_9$ and $SbW_{14}$. FTIR (top) and Raman (bottom) spectra comparing the $SbW_{14}$ (orange curves) with the starting material, $SbW_9$ (purple curves). *Residual ethanol from crystal and sample holder washing.

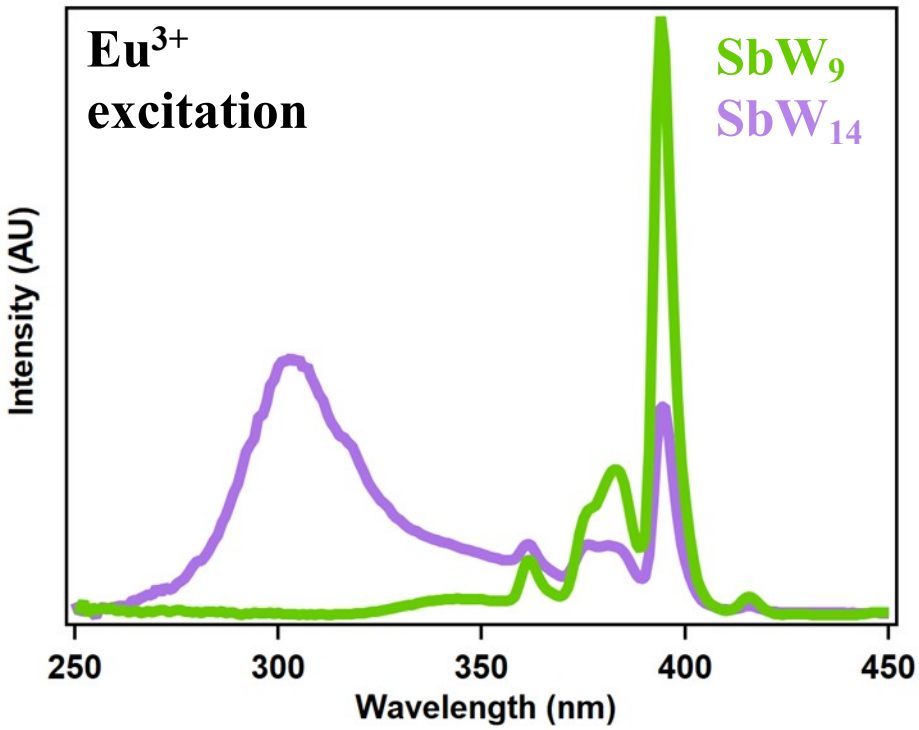


Figure S2. $Eu^{3+}$ excitation spectrum. $SbW_9$ in green, $SbW_{14}$ in purple. Note how the excitation pathways are different for $SbW_9$ vs. $SbW_{14}$. Preferential sensitization via the POM and intramolecular energy transfer to $Eu^{3+}$ is observed for $SbW_{14}$. However, for $SbW_9$ direct excitation of the POM-bound $Eu^{3+}$ is more efficient. Solution conditions were as follows: [Eu] = 1 mM, [$SbW_9$] and [$SbW_{14}$] = 2 mM, dissolved in acetate buffer at pH of 5.5. Emission wavelength 615 nm, emission and excitation slits both at 4 nm.

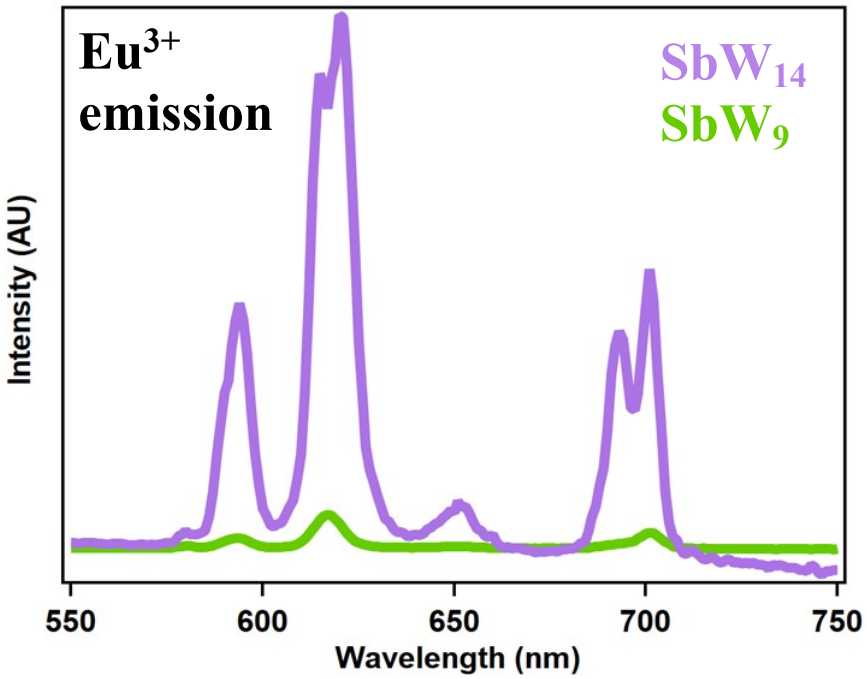


Figure S3. $Eu^{3+}$ emission spectrum. $SbW_9$ in green, $SbW_{14}$ in purple. [Eu] = 1 mM, [$SbW_9$] and [$SbW_{14}$] = 2 mM, dissolved in acetate buffer at pH of 5.5. Excitation wavelength 303 and 343 nm, emission and excitation slits both at 4 nm

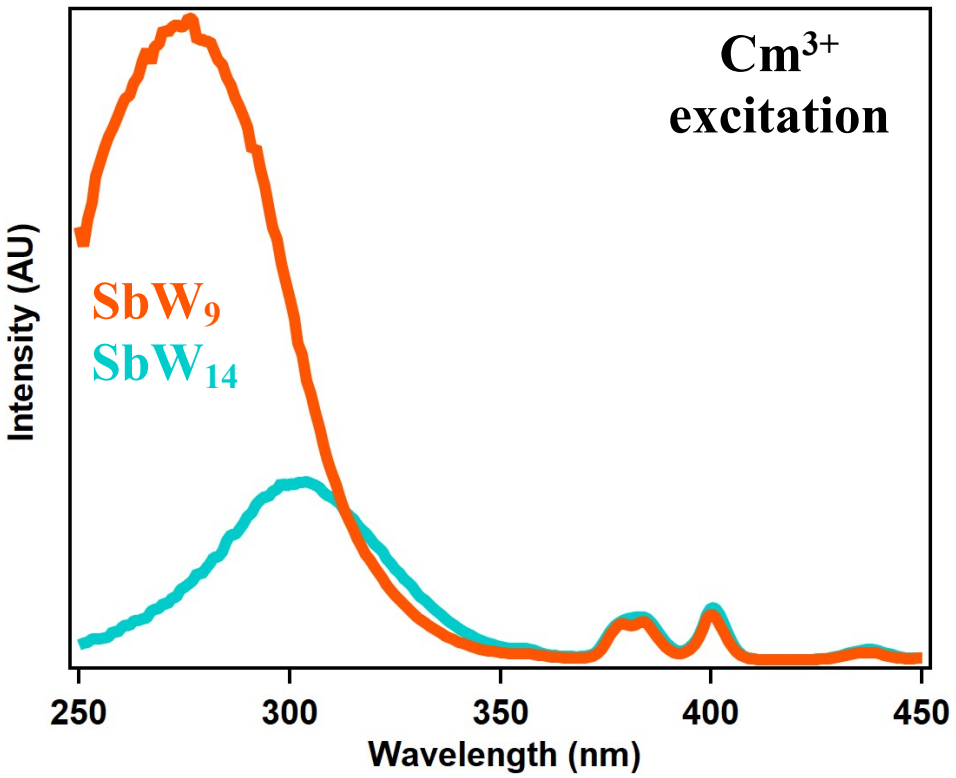


Figure S4. $Cm^{3+}$ excitation spectra. $SbW_9$ in orange, $SbW_{14}$ in blue. [Cm] = 100 µM, [$SbW_9$] and [$SbW_{14}$] = 200 µM, dissolved in acetate buffer at pH of 5.5. Emission wavelength 605 nm, emission and excitation slits both at 4 nm

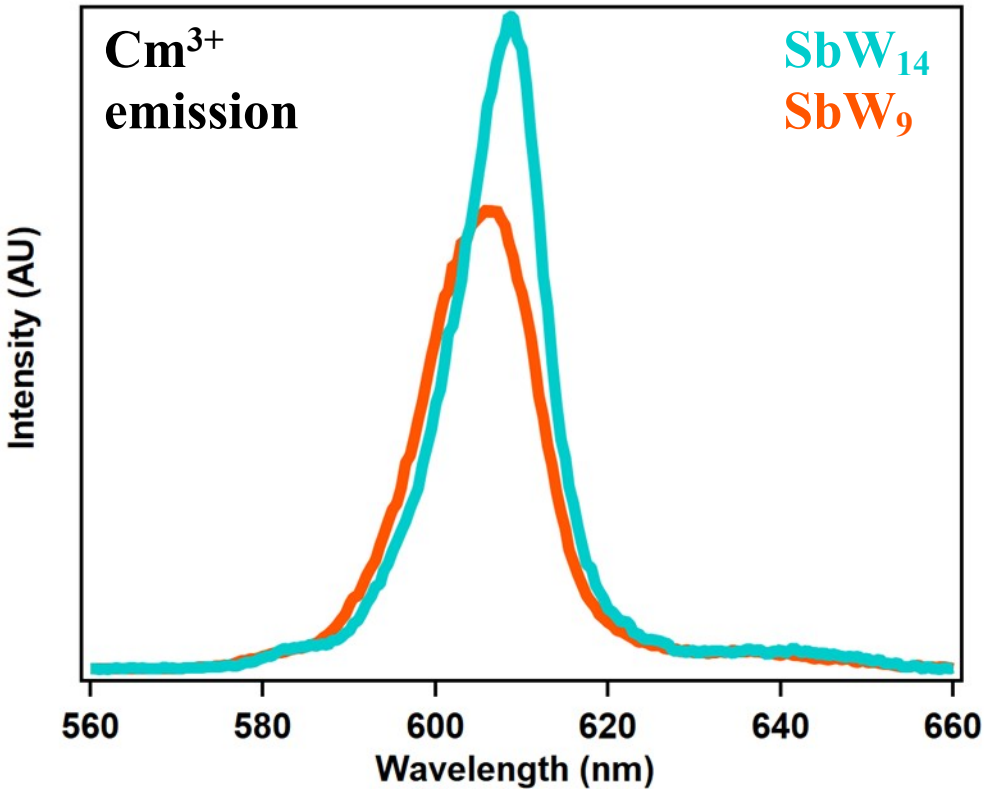


Figure S5. $Cm^{3+}$ emission spectra. $SbW_9$ in orange, $SbW_{14}$ in blue. [Cm] = 100 µM, [$SbW_9$] and [$SbW_{14}$] = 200 µM, dissolved in acetate buffer at pH of 5.5. Excitation wavelength 273 and 303 nm, emission and excitation slits both at 4 nm

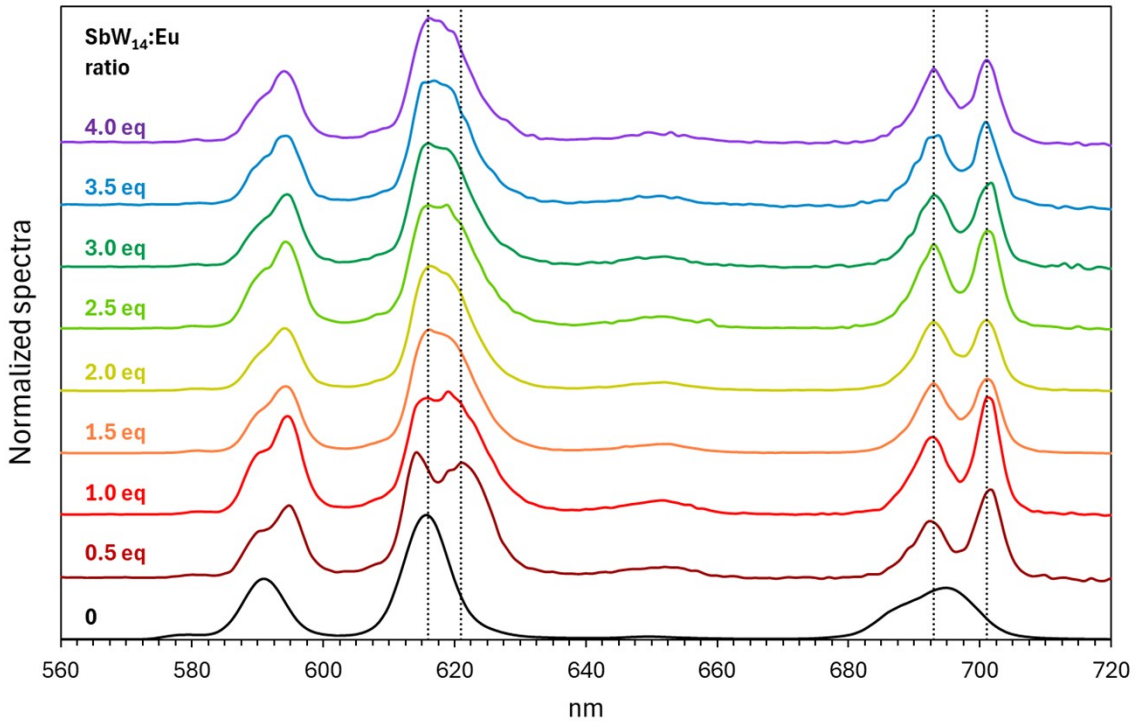


Figure S6. Fluorescence emission spectra of Eu3+ in the presence of SbW14 and as a function of the ratio $SbW_{14}$/Eu. pH = 5.5 (0.1 M acetate buffer). [Eu] = 1 mM. The molar ratio $SbW_{14}$/Eu is indicated above each spectrum. The vertical lines are for eye guidance and to highlight the spectra changes at 614, 621, 693, and 701 nm. The spectral changes occur between 0 and 2 equivalents of POM and then the spectrum stabilizes.

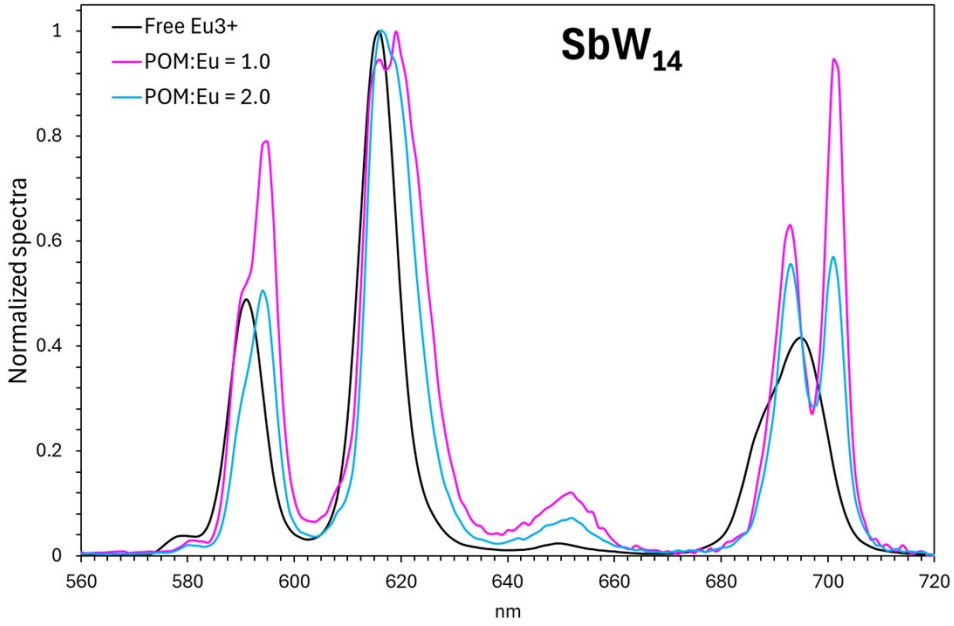


Figure S7. Comparison of the Eu fluorescence spectra for $Eu^{3+}$ without POM (black curve), with 1 equivalent of $SbW_{14}$ (pink curve), and 2 equivalents of $SbW_{14}$ (blue curve).

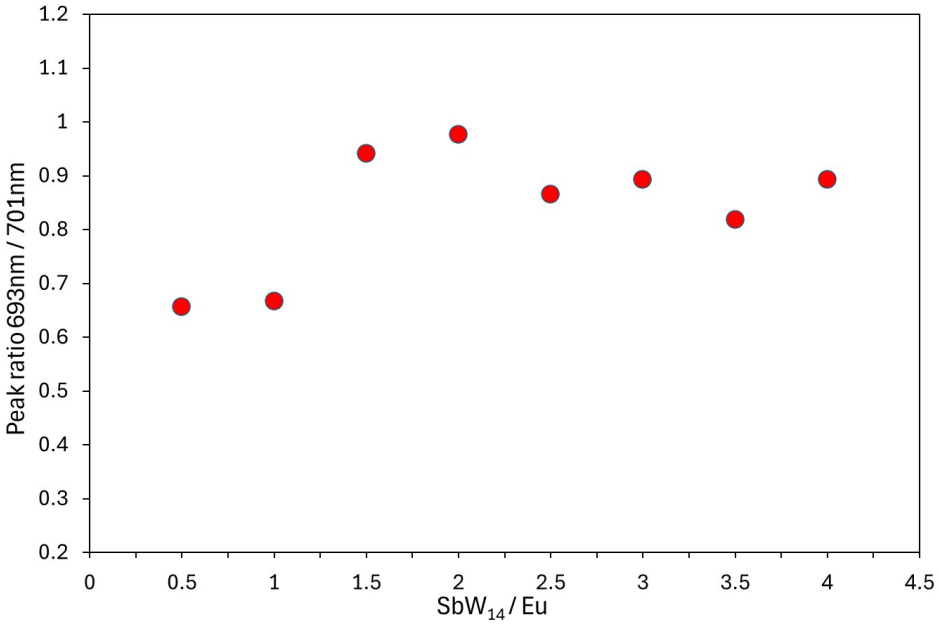


Figure S8. Ratio of the fluorescence peak intensities at 693 nm over 701 nm (see Figure S7 for full spectra).

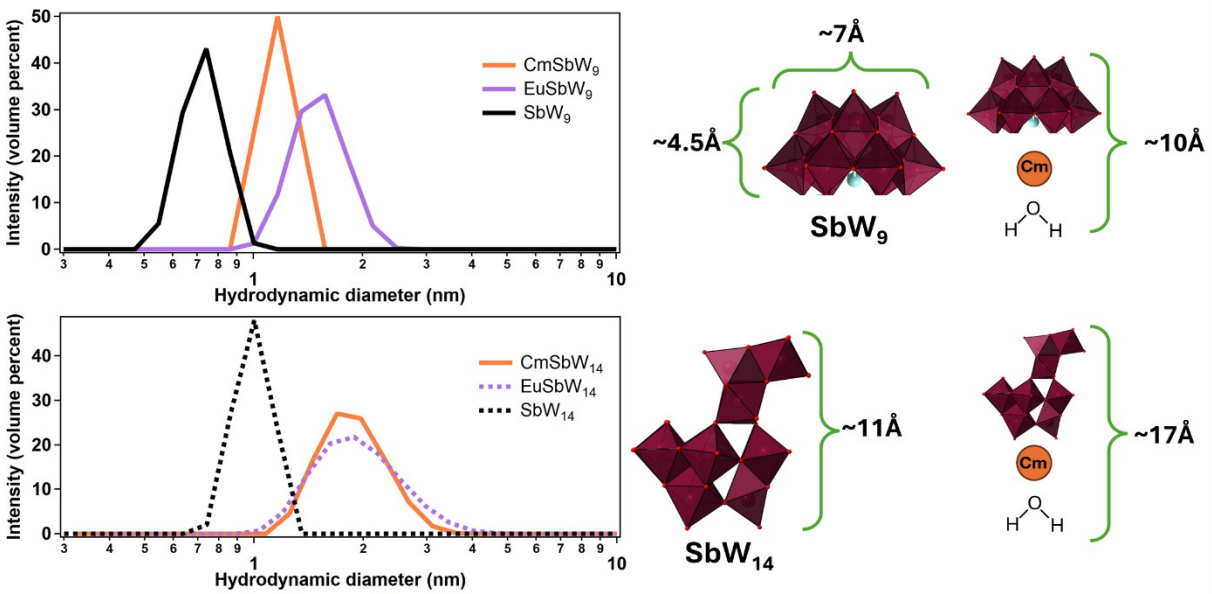


Figure S9. Dynamic Light scattering for $SbW_9$ (top panel) and $SbW_{14}$ (bottom panel) with Eu (purple) and Cm (orange). On the right side, distances for uncomplexed $SbW_9$ and $SbW_{14}$ are based on single crystal structures. The Cm-POM complexes are hypothetical, and their hydrodynamic sizes were estimated from the POM size and the typical length of a Cm-O bond (i.e., 2.4-2.5 Å).[13] The DLS curves seem consistent with the formation of 1:1 complexes. However, note that ion pairing between the POM complexes and $Cs^+$ counterions could increase the observed hydrodynamic sizes so the assignment here is tentative.

Table S5. Dynamic Light Scattering Results.

| | *Hydrodynamic diameter (Å)* | *Hydrodynamic diameter (nm)* | *Standard Deviation (nm)* |
|---|---|---|---|
| **$SbW_9$** | 7.37 | 0.737 | 0.101 |
| **$SbW_9$-Eu** | 16.08 | 1.608 | 0.110 |
| **$SbW_9$-Cm** | 11.67 | 1.167 | 0.140 |
| | | | |
| **$SbW_{14}$** | 11.13 | 1.113 | 0.115 |
| **$SbW_{14}$-Eu** | 20.05 | 2.005 | 0.129 |
| **$SbW_{14}$-Cm** | 19.45 | 1.945 | 0.147 |

**References**


1) Bösing, M., Loose, I., Pohlmann, H. and Krebs, B. (1997), New Strategies for the Generation of Large Heteropolymetalate Clusters: The β-*B*-$SbW_9$ Fragment as a Multifunctional Unit. Chemistry – A European Journal, 3: 1232-1237.

2) Feng Chai, YiPing Chen, Zhen Yang, LiuQin Su, YanQiong Sun, Synthesis and characterization of a new Hervé-type tungstoantimonite based on α-[SbW9O33]9− unit, Journal of Molecular Structure, 1051, 2013, 101-106,

3)Sheldrick, G. M. Bruker-Siemens Area Detection Absorption Other Correction; 2008.

4) Sheldrick, G. M. SHELXT – Integrated Space-Group and Crystal-Structure Determination. Acta Cryst A 2015, 71 (1), 3–8. https://doi.org/10.1107/S2053273314026370.

5) Sheldrick, G. M. A Short History of SHELX. Acta Cryst A 2008, 64 (1), 112–122. https://doi.org/10.1107/S0108767307043930.

6) Dolomanov, O. V.; Bourhis, L. J.; Gildea, R. J.; Howard, J. a. K.; Puschmann, H. OLEX2: A Complete Structure Solution, Refinement and Analysis Program. *J Appl Cryst* **2009**, *42* (2), 339–341. https://doi.org/10.1107/S0021889808042726.

7) Van Der Sluis, P. & Spek, A. L. BYPASS: an effective method for the refinement of crystal structures containing disordered solvent regions. Acta Crystallographica Section A 46, 194–201 (1990).

8) Glasser, L. The effective volumes of waters of crystallization: non-ionic pharmaceutical systems. Acta Cryst B 75, 784–787 (2019).

9) Glasser, L. Effective Volumes of Waters of Crystallization: Ionic Systems. Crystal Growth & Design 19, 3397–3401 (2019).

10) Massa, W., & Gould, R. O. (2016). Crystal structure determination (2nd ed.). BoD, Books on Demand

11) Brese and O'Keeffe, (1991), Acta Cryst. B47, 192-197 (extrapolated)

12) Sidey (2009) Acta Cryst, B65, 99-101

13) Skanthakumar S., Antonio M. R., Wilson R. E., Soderholm L. The curium aqua ion. Inorg. Chem. 2007, 46, 9, 3485–3491